Static Stability and Seismic Behavior of the Dome of the Hagia Sophia

By

Ali Irani

B.S. Architecture
B.S. Civil and Environmental Engineering
Massachusetts Institute of Technology, 2016

SUBMITTED TO THE DEPARTMENT OF CIVIL AND ENVIRONMENTAL ENGINEERING IN PARTIAL FULFILLMENT OF THE REQUIREMENTS FOR THE DEGREE OF

MASTER OF ENGINEERING IN CIVIL ENGINEERING
AT THE
MASSACHUSETTS INSTITUTE OF TECHNOLOGY

JUNE 2017

Signature redacted

Signature of Author: _____
Department of Civil and Environmental Engineering
May 12th, 2017

Signature redacted

Certified By: _____
John Ochsendorf
Class of 1942 Professor of Architecture and Civil and Environmental Engineering
Thesis Supervisor

Signature redacted

Accepted By: _____
Jesse Kroll
Associate Professor of Civil and Environmental Engineering
Chair, Graduate Program Committee

Static Stability and Seismic Behavior of the Dome of the Hagia Sophia

By

Ali Irani

Submitted to the Department of Civil and Environmental Engineering on
May 12, 2017 in partial fulfillment of the requirements for the Degree of
Master of Engineering in Civil Engineering

Abstract

The Hagia Sophia in Istanbul represents a culmination of engineering practice and design aesthetics that were emulated extensively by both Byzantine and Ottoman builders. The resiliency and scale of the brick masonry dome of the Hagia Sophia, particularly with respect to its seismically active location, is a testament to the iterative and empirical construction techniques of its constructors. The existing analyses of the structure have focused primarily on architectural features as well as seismic response using various computational implementations of the Finite Element Method (FEM). This thesis seeks to better understand the static stability of the Hagia Sophia dome and its dynamic failure mechanisms through a combination of analytical and experimental techniques. By utilizing limit analysis, implemented through graphical methods, the stability of the dome can be calculated by assuming the compression-only behavior of masonry. This analysis demonstrates that the horizontal thrust of the dome is 275 kN and the vertical thrust is 1012 kN. Experimentally, a scaled and discretized 3D printed model of the Hagia Sophia dome was tested to find that the minimum lateral ground acceleration necessary to cause collapse is 0.725g. In addition, the minimum outward displacement of supports necessary to induce failure was determined to be 2.1m. The analysis undertaken in this thesis will ultimately inform the maintenance and restoration of the dome and help provide design and structural precedents for masonry construction of large diameter domes.

Thesis Supervisor: John Ochsendorf

Title: Class of 1942 Professor of Architecture and Civil and Environmental Engineering

Table of Contents

	Acknowledgements	6
I.	Introduction	
	1. *Background on the Hagia Sophia*	7
	2. *Overview and Investigation*	7
II.	Literature Review	
	1. *Theories of Masonry Analysis*	9
	2. *Computational Methods*	9
	3. *Limit Analysis*	10
	4. *Membrane Analysis*	10
	5. *Graphic Statics*	11
	6. *Scale Models and Physical Experimentation*	11
III.	Methodology	
	1. *Model Generation*	13
	2. *Material Study*	13
	3. *Implementation of Graphic Statics*	14
	4. *Scaled Model and 3D Printing*	16
	5. *Tilting Test*	17
	6. *Spreading Test*	18
IV.	Results and Discussion	
	1. *Comparison of Hoop and Meridional Forces*	19
	2. *Overturning Stability of the Dome of the Hagia Sophia*	20
	3. *Comparison to Other Methods*	20
	4. *Comparison to Later Ottoman Domes*	21
	5. *Collapse Due to Seismic Activity*	22
	6. *Collapse Due to Displacement of Supports*	24
V.	Conclusions	26
VI.	Appendix A – Graphic Statics Theory and Implementation	28
VII.	Appendix B – Python Scripts	29
VIII.	Bibliography	36

List of Figures and Tables

Figures

1 – 3D Model and Annotated Drawing of Hagia Sophia 13
2 – Meridional and Hoop Forces on an Idealized Dome 14
3 – Division of an Idealized Dome into Lunes 14
4 – Process Logic for Implementation of Graphic Statics 15
5 – Process Logic for Discretization of Dome 16
6 – Tilting of an Idealized Dome 17
7 – Spreading of an Idealized Dome 18
8 – Thrust Line Solutions for the Dome of the Hagia Sophia 19
9 – Factor of Safety against Overturning for the Dome of the Hagia Sophia 20
10 – Thrust Line Solutions for the Hagia Sophia and 2 Ottoman Domes 21
11 – Tilt Table Collapse: 9 Frames 22
12 – Graphic Statics Solution for Tilting Collapse 23
13 – Spreading Table Collapse: 9 Frames 24

A1 – Theory and Basic Development of Graphic Statics 28

Tables

1 – Thrust Values for the Dome of the Hagia Sophia 19
2 – Safety Factors against Overturning for Piers of the Hagia Sophia 20
3 – Static Stability and Thrust of the dome of the Hagia Sophia and Ottoman Domes 21
4 – Experimental Values of Lateral Ground Acceleration Using Tilting Test 22
5 – Experimental Values for the Outward Spread Distance 24

Acknowledgements

The completion of this M.Eng thesis represents the culmination, and ultimately conclusion, of my 5 years at MIT. Through my undergraduate and later graduate career, I have been consistently challenged, frustrated, enthralled, and overjoyed by the shear wealth of knowledge and opportunities available at this institution. I have had the helping hand and gentle guidance of many faculty members. But one person, in particular, is worthy of special mention and acknowledgement.

I first met John Ochsendorf during my first year at MIT and our work together has taken us through the domains of architecture, engineering, and history. In classes and research projects, he has helped me explore everything from Gothic cathedrals and medieval Iranian domes to high-rise towers, bridges, and shells. He considers the great engineers and architects of the past to be our best mentors and he admires simplicity in concept and implementation. His enthusiasm and endless expertise continues to inspire me and I am indebted to him for all he has taught me and the lessons I will greatly cherish. It is only fitting that I end my MIT career with an investigation of one the great, historic buildings of the world, the Hagia Sophia, which continues to amaze and inspire 1500 years after its construction.

I particularly want to thank Marcin Szyszka, a visiting Fulbright student from Wroclaw University of Science and Technology for his incredible help and support. Marcin was instrumental in the success of this project and helped guide me through experimental setups and rigorous analytical checks. But perhaps, more importantly, he is a great friend who was always willing to listen and lend a hand.

Stephen Rudolph was an invaluable source of ideas and assistance throughout this investigation and I would like to acknowledge him for his significant contributions to the experimental part of this study. I would like to also thank Dr. James Bales of the Edgerton Center for his input on high speed footage recording.

And finally I would like to thank everyone in the M.Eng program and the larger Civil and Environmental Engineering community at MIT for their friendship and eagerness to help and innovate.

I - Introduction

1.1 - Background on the Hagia Sophia

Originally constructed between the years 532-537 CE, the Hagia Sophia was commissioned by Justinian I, the Byzantine emperor, to be his imperial church in Constantinople. The design for the first church was developed by Isidore of Miletus and Anthemius of Tralles, who were chose by Justinian to serve as the architects for the project. As the seat of the Orthodox patriarch in Constantinople, it was the location for all imperial Byzantine ceremonies, such as coronations (Mark and Cakmak 1992). The original dome was noted to be very flat compared to the current configuration and earthquakes in 553, 557, and 558 CE caused major cracking and the ultimate collapse of the main dome. The reconstructed dome (completed in 562 CE) was higher than the original (the Hagia Sophia has a current height of 55 meters) and was supported by four pendentives (Mark and Cakmak 1992). An earthquake in 989 CE caused a partial collapse of the dome, at which time, the main dome was reconstructed. These repairs were ultimately completed in the year 994 CE under the direction of Emperor Basil II. The constant renovations on the dome, in response to earthquakes during this period of time, ultimately gave the dome its current asymmetry with a variable diameter roughly equivalent to 32 meters. In the year 1317, four massive buttresses were added to the Hagia Sophia, to further stabilize the dome (Mark and Cakmak 1992). At this point, however, the Hagia Sophia was in a poor state, as a result of the political faltering of the Byzantine Empire.

After the capture of Constantinople by Ottoman forces under Mehmet II, in 1453, the Hagia Sophia was converted into a mosque. This was accompanied by some renovations. Minarets were added to the structure during the reigns of Sultan Bayezid II (1481-1512), Suleiman I (1520-1566), and Selim II (1566-1574). It was during the reign of the latter sultan, that significant retrofits were made to the structure of the Hagia Sophia. These constructions were undertaken by the principal Ottoman architect and engineer at the time, Sinan. Sinan's renovations included stabilizing the foundation, clearing the site of houses and other outbuildings, repairing cracks in the dome, and perhaps, most significantly, the addition of four flying buttresses to resist the outward spread of the dome. These buttresses are recorded in an engraving by Melchior Lorck, a Danish painter and printmaker, from the year 1559 (Mark and Cakmak 1992). The other imperial Ottoman mosques designed and built by Sinan all employ the characteristic flying buttresses and it seems only natural that Sinan used a similar stabilizing technique on the quickly deteriorating Hagia Sophia.

Under the reign of Sultan Abdulmecid I, in the year 1847, the Swiss-Italian architects Gaspare and Giuseppe Fossati were tasked with repairing the building and restoring its mosaics (Mark and Cakmak 1992). The Fossati brothers removed the flying buttresses added by Sinan and instead used an iron chain at the base of the dome to resist the outward movement which had been causing significant cracking. After the renovations of 1847-49, no other significant retrofits were undertaken until 1997. Completed in 2006, the most recent renovations to the building repaired cracks in the dome and restored many of the interior details and aesthetics (World Monuments Fund 2017).

1.2 - Overview of Investigation

The study and analysis of historic masonry structures is of utmost importance to the effective restoration and preservation of these heritage structures. In many seismically active regions of the world, masonry structures such as domes are in danger of collapsing or being reinforced in ways which may hasten their failure. This is primarily due to a lack of understanding of the fundamental behavior of masonry as well as the stability and failure mechanisms associated with these structures. As one of the hallmarks of Byzantine design, and a prominent world architectural monument, the Hagia Sophia, and

most importantly its dome, is one such masonry structure that has endured multiple seismic events and several changes of political power. This investigation seeks to better understand the static stability of the current dome of the Hagia Sophia and explore how the dome fails in response to seismic activity and support movements. Special focus is given to the dome, as opposed to the entire building, due to its significant structural role and vulnerability to failure. Based on the results of this investigation, a better understanding and awareness of the behavior of large, masonry domes is developed which can be instrumental in their subsequent repair and restoration.

II - Literature Review

There are multiple analytical, computational, and experimental methods for describing the behavior of historical masonry structures. Many of these methods have been used to provide some level of structural analysis for either the dome or the entirety of the Hagia Sophia. Each methodology has its own key assumptions, and ultimately some are better suited to describe the fundamental behavior of masonry.

2.1 - Theories of Masonry Analysis

Masonry structures can either be analyzed using elastic or limit analysis. First outlined by Navier (1826), elastic analysis assumes that the material is a continuum, homogenous and isotropic, and that deformations are small. However, this analysis is inconsistent with masonry structures, which are composed of discrete, heterogeneous stones or brick which are separated by a joint or a crack. In addition, the deformations associated with the overall masonry structures are quite large, and often visibly noticeable. To this end, the limit analysis of masonry structures seeks to better approximate the behavior of masonry, by making three key material assumptions, formalized by Jacques Heyman (1997):

1. Masonry has infinite compressive strength
2. Masonry has no tensile strength
3. Sliding failure does not occur

Given the relatively low stresses in masonry structures, the first assumption is valid. In addition, while a brick or stone may be able to be loaded in tension, the joints cannot be loaded (mortar is too brittle to sustain any tensile forces). Furthermore, it is often correct to assume that the high coefficient of friction between blocks prevents sliding failure. Thus, analysis of masonry structures becomes not about strength and elasticity, but more about stability (Zessin 2012).

2.2 - Computational Methods

In the field of elastic analysis, to date, several computational, finite element models (FEM) of the Hagia Sophia have been constructed (Mark et al. 1995). Typically, all of these models evaluated the entire building, not just the dome. These simulations approximate the early phase behavior of the mortar in an attempt to derive a general form for the constitutive behavior of the masonry. These models have found the horizontal and vertical thrust associated with the dome as well as the average deformation in the main piers and arches of the Hagia Sophia (Swan and Cakmak 1993). Further FEM analysis of the building has introduced seismic accelerations, associated with historical earthquake events, and examined the behavior of the Hagia Sophia in response to these. Typical results associated with this seismic analysis include natural frequencies and mode shapes of the building (Cakmak et al. 1993).

However, these FEM simulations make several key assumptions which limit their applicability. Primarily, FEM analysis assumes some degree of elastic behavior in the medium. These models assume that this elasticity can be derived from the supposed tensile strength of the mortar between the bricks. Although the mortar may be stiff enough in some regions, often it is too dry and brittle to sustain any tension load. Cracking patterns in masonry domes also invalidate any consideration of mortar strength; the dome is cracked so there are no more mortared contact surfaces between certain segments, yet the dome is still stable.

Furthermore, many of these computational models use calibration from in-situ measurements. While this technique ensures that results are realistic, it does not prove the applicability of the model for masonry analysis.

Perhaps even more importantly, FEM analysis is unable to simulate collapse mechanisms or simulate required failure loads or accelerations due to seismic events. Since one of the key assumptions in elastic analysis is small deformation, these computational models cannot account for the large displacement, cracking, and hinging typically associated with masonry structures.

More recent FEM analysis of the Hagia Sophia has taken advantage of improvements in modeling assumptions and deployed more advanced non-linear analysis to the entirety of the structure (Almac et al. 2013). In addition, there is the possibility of using discrete element modeling (DEM) analysis to simulate the behavior of masonry structures. DEM analysis better accounts for the criteria determining the stability of masonry by using physics based, rigid-body motion analysis, not accounting for significant deformation. Nonetheless, advanced FEM and DEM analysis of large buildings is incredibly complex, time consuming, and expensive, making this type of modeling out of the scope for most restoration and retrofit projects.

2.3 - Limit Analysis

Contrasting with FEM elastic analysis, limit analysis of masonry structures is primarily concerned with the stability of the blocks or units which can be evaluated via a line of thrust, a locus of points along which internal forces (resultant compressive forces) flow. The two following theorems dictate the stability and failure mechanisms associated with masonry structures.

1. *Safe Theorem:* If a line of thrust can be found which is in equilibrium with the external loads and which lies wholly within the masonry, the structure is safe (Heyman 1997).

2. *Uniqueness Theorem*: If a line of thrust can be found which represents an equilibrium state for the structure under the action of the given external loads, which lies wholly within the masonry, and which allows the formation of sufficient hinges to transform the structure into a mechanism, then the structure is on the point of collapse (Heyman 1997).

For uniform thickness and hemispherical geometries, the line of thrust can be derived analytically. This is particularly useful, as the location of hinges and associated displacements can be found. This implementation of limit analysis has been developed to consider the stability of the dome of the Hagia Sophia (Pavlovic et al. 2016). While the failure mechanisms found in this investigation are correct, the study considers a single point load as the cause for collapse. This is unrealistic as it is hard to imagine a source that could impart such a high magnitude force onto the dome. In addition, while it is convenient to assume that a dome is uniform in thickness and hemispherical, this is a large simplification for a structure with highly variable geometry such as the Hagia Sophia.

2.4 - Membrane Analysis

Membrane theory, as a particular implementation of limit analysis, is useful in the evaluation of masonry domes since it assumes that applied loads are only resisted by internal forces in pure compression. In effect, membrane analysis assumes a zero-thickness surface that has no stiffness to bending. Membrane analysis also dictates that forces act in the latitudinal (meridional) or hoop directions and equilibrium solutions are constrained to the median surface of domes. The dome of the Hagia Sophia has been analyzed using this technique (Duppel 2009). This investigation provides values for the horizontal and vertical thrust associated with the dome. However, in general, membrane theory often underestimates dome stability since only solutions constrained to the centerline of the structure are considered. Logistically, it is often difficult to apply the relevant equations to non-uniform geometries.

2.5 - Graphic Statics

Graphical implementations of limit analysis can also be developed based on the fundamental assumptions of masonry behavior. Graphic statics, a particular method formalized by Karl Culmann (1864), can be used to analyze the stability of structure by demonstrating the link between the internal forces and line of thrust for a structure. This method is based on the representation of forces as vectors and finding equilibrium states.

One of the earliest masonry structures to be analyzed using graphic statics was the dome of St. Peter's basilica (Poleni 1748). By considering the dome as a series of independent wedges or *lunes*, Poleni only considered downward latitudinal or meridional forces. This did not account for hoop forces acting between the lunes and so it is a conservative estimate of the dome's stability.

Wolfe (1921) refined graphic statics to account for both hoop and meridional forces in the analysis of domes. The implementation is similar to membrane theory, however it allows for the line of thrust to depart from the median of the surface in certain locations. This was further developed by Lau (2006).

One key problem with graphical methods is that they are tedious and time consuming to implement by hand. However, with the advent of parametric modeling and other computational tools, graphical methods can readily be applied to non-uniform thickness masonry structures (Block 2005). Nonetheless, to date, there has been no graphic statics analysis of the Hagia Sophia or any other later era Ottoman domes. The development of quick and adaptable graphical methods will be a key contribution of this investigation as it seeks to answer the following research question:

1. *What does limit analysis, implemented via graphic statics, reveal about the structural behavior and performance of historical masonry domes, in particular the Hagia Sophia?*

2.6 - Scale Models and Physical Experimentation

The use of scale models to test the collapse behavior of masonry structures is a nascent field. Much of this work has historically focused on arches with limited work on other masonry structures. Zessin et al. (2010) and Quinonez et al. (2010) developed the use of 3D printed domes to evaluate their performance under quasi-dynamic conditions. These hemispherical, uniform thickness domes were constructed out of multiple 3D printed gypsum blocks which were subsequently coated with polyurethane adhesive to aid in model durability. Two important physical experiments were conducted on these domes:

1. Tilting Test: By placing the dome on a surface that can be gradually tilted, the angle of collapse can be measured. This angle can then be correlated to the minimum ground acceleration required to collapse the dome (DeJong 2009; Zessin 2012). This is a direct measure of the strength of a given seismic event.
2. Spreading Test: By placing the dome on a series of spreading leaves, the minimum outward movement of supports needed to induce a collapse mechanism can be experimentally derived. By applying a scaling factor, the relevant value for the full scale dome can be found (Zessin et al. 2010; Zessin 2012).

This investigation seeks to better understand the possible collapse behavior of the Hagia Sophia by developing a similar 3D printed model and repeating the two tests in order to answer these two research questions:

1. *With regards to seismic performance, what is the minimum lateral ground acceleration necessary to collapse the dome of the Hagia Sophia?*
2. *What is the qualitative behavior of the Hagia Sophia in response to moving supports and what is the minimum outward movement required to induce a collapse mechanism?*

III - Methodology

In order to better understand the behavior of the Hagia Sophia and answer the three main research questions reviewed in Sections 2.5-6, this investigation utilized both a computational implementation of graphic statics as well as scaled, experimental model of the dome. The procedure for the development of the analytical and experimental phases of this investigation are explored in this section.

3.1 - Model Generation

The model of the dome of the Hagia Sophia was based on section cuts of the structure (Necipoglu 2005). The drawings were prepared using Rhinoceros 3D (see Figure (1)), a commercially available 3D modeling platform (Robert McNeel and Associates 2012). Previous investigations focused on the entirety of the structure of the Hagia Sophia. This is a logistical constraint on the development of quick analysis and scaled experimental models. This investigation chose to focus solely on the dome. This is justified for two primary reasons. First, the dome is the largest single-spanning element in the Hagia Sophia and is thus, of primary interest in the investigation of static and seismic stability. In addition, the rest of the Hagia Sophia is incredibly massive and stable due to the built up construction of additional retaining and buttressing walls. Relatively considered, the dome is very light and so there is much greater concern about its behavior relative to the whole building. Secondly, the historical earthquakes that have occurred at the site all either completely or partially collapsed the dome while other structural elements such as half domes and arches may or may not have been damaged. This validates the idea that the dome is indeed the most critical and weakest structural component of the building.

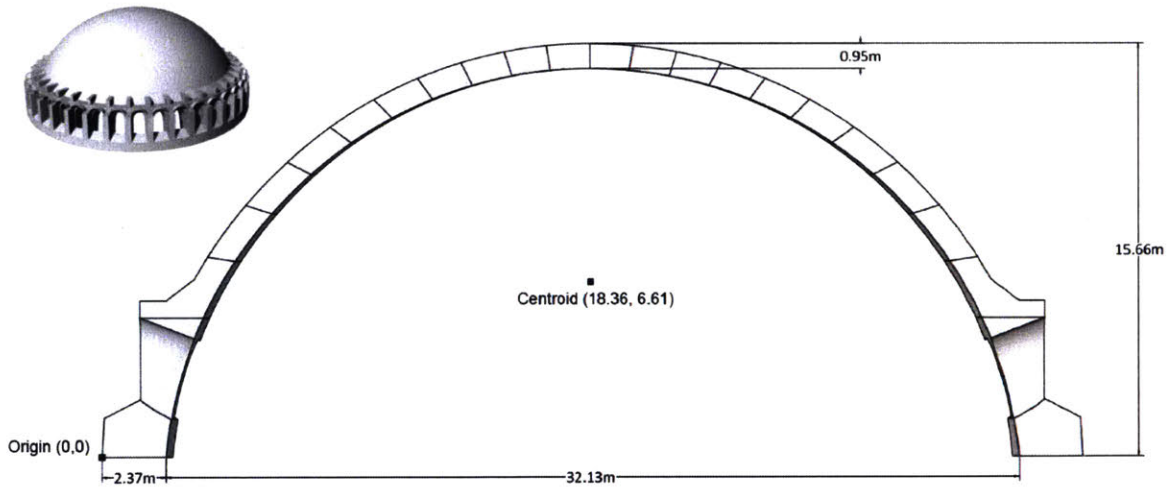

Figure (1): Rhino 3D model of the dome and annotated section through the dome indicating key dimensions.

3.2 - Material Study

The dome of the Hagia Sophia is constructed out of bricks with layers of mortar between them. An investigation of the mechanical and chemical properties of the bricks reveals that they have a density of 1540 kg/m^3 and that the mortar has a density of 1430 kg/m^3 (Mark and Cakmak 1994). Nonetheless, a density of 1700 kg/m^3 is used by some computational simulations (Swan and Cakmak 1993) and a density of 1843 kg/m^3 is considered in a membrane theory analysis of the dome (Duppel 2009). This investigation will consider the latter two densities in order to be able to effectively compare its findings with previous studies.

3.3 - Implementation of Graphic Statics

3.3.1 - Graphic Statics and Application to 3D Geometry

Graphic statics is a vector equilibrium implementation of limit analysis that is readily applicable to two-dimensional structures such as arches. These specific structures are held in a static equilibrium solely via downward compressive or meridional forces. An overview of this analysis method and a small example are provided in Appendix A of this thesis.

Three dimensional masonry structures such as domes involves both meridional forces as well as longitudinal hoop forces (see Figure (2)).

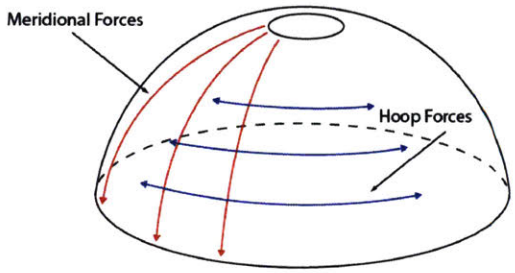

Figure (2): Meridional and hoop forces acting on an idealized dome.

As demonstrated by Poleni (1748), the graphic statics analysis of masonry domes must decompose the structure into wedges or *lunes*. Figure (3) indicates how a hemispherical dome is cut into 16 slices of 22.5° each. The lune effectively serves as a two-dimensional representation of the dome since the magnitude of self-weight dramatically reduces towards the top of the lune. Appropriate lune angles range from 10-15°. By considering only the meridional forces (i.e. each lune acting independently), a similar approach to Figure (2) can be used to generate the thrust line for a dome once the lune is divided into individual voussoirs.

Wolfe (1921) developed a modified thrust line method to account for the hoop forces in the dome. This is a conservative method that makes one critical assumption: for a hemispherical dome, at about 52° from the horizontal, the hoop forces change in direction. Above this angle, the upper half of the dome is held together both by the compressive meridional forces as well as compressive hoop forces. To account for the contribution of the hoop forces, Wolfe's modified thrust line is constrained to the median surface of the lune for this region. Based on a series of vector relations, the magnitude of the hoop forces can also be derived. The lower half of the dome, however is only held together by meridional forces since the hoop forces are tensile in this region. Since it can be assumed that masonry has no tensile capacity, the analysis of the lower part of the dome is the standard two-dimensional graphic statics approach.

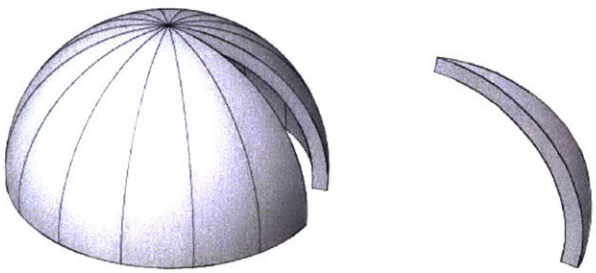

Figure (3): Idealized hemispherical dome divided into lunes. The removed slice indicates the wedge like geometry of the lune which is essential for the accurate implementation of graphic statics.

3.3.2 - Computational Implementation

This investigation has focused on developing a robust, computational implementation of graphic statics that is able to account for both hoop and meridional forces in domes with variable geometry and non-uniform thickness.

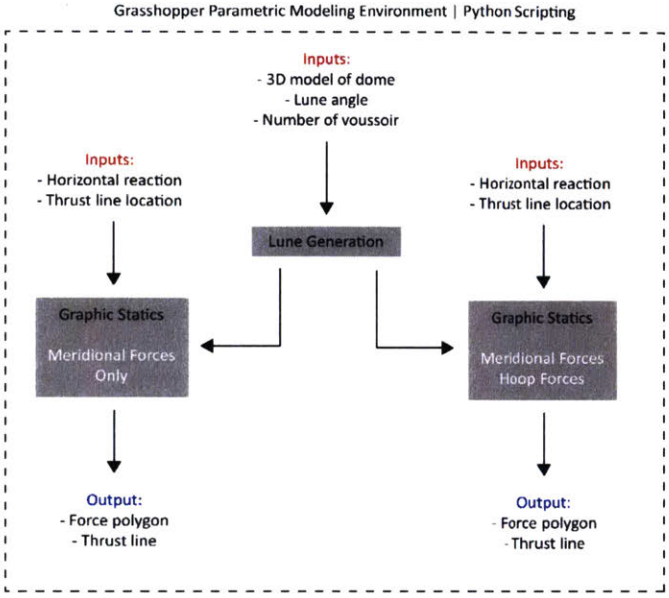

Figure (4); Process logic for the implementation of graphic statics for a given dome geometry within the Rhinoceros 3D and Grasshopper modeling environment.

Since graphic statics is essentially an iterative method, tasked with finding an admissible line of thrust for a structure, it is an ideal use of the flexibility afforded by parametric modeling. Given that the model of the Hagia Sophia dome was prepared using Rhinoceros 3D, it is natural to use the associated plugin, Grasshopper, to develop the graphic statics solutions for the dome. Grasshopper is a visual programming language that interacts and ties with the core functions of Rhinoceros 3D which allows parametric control of geometry. Grasshopper also allows a user to develop custom Python scripts which afford even greater control over Rhinoceros 3D geometry (Robert McNeel and Associates 2014).

The process logic for the implementation of graphic statics is illustrated in Figure (4). The following steps are involved in the implementation of graphic statics in Grasshopper via the Python programming language.

1. Lune Generation: The 3D model of the dome is divided and one lune, with the desired input angle, is output. The number of voussoirs is also input, as a parameter, which splits one lune into multiple blocks.
2. Graphic Statics (Meridional Forces Only):
    a. The volume of each voussoir is calculated and a load line is generated based on an input density for the blocks.
    b. Based on the input horizontal reaction, the force polygon is constructed.
    c. The line of thrust is generated based on the geometry of the force polygon (see section 3.3.1) and the line is superimposed onto the geometry of the lune. A series of inputs control the starting point of the thrust line.
    d. The horizontal reaction is another parametric control that can be modified to ensure that the line of thrust fits completely within the structure.
3. Graphic Statics (Meridional and Hoop Forces)
    a. The same procedure is repeated to generate the load line for the dome.

b. For the blocks above the critical angle (an input), the line of thrust is constrained to the centerline of the lune, which can be extracted from the 3D geometry.
c. For the blocks below the critical angle, the horizontal reaction force is an input. Based on this, the entire force polygon is constructed.
d. The same series of controls (horizontal reaction, starting location) can be iteratively changed to ensure that the thrust line is admissible for the given dome geometry.

This particular methodology is an important contribution of this investigation. Since this particular implementation of graphic statics uses a complete 3D model for the dome, as opposed to only accepting a lune input, and requires minimum inputs, it is able to generate the line of thrusts for domes of varied geometries and with non-uniform thicknesses. Therefore, simplifications are not necessary and a more accurate evaluation of the stability and internal forces of the dome can be produced.

3.4 - Scaled Model and 3D Printing

An accurate scaled model of a masonry structure must best reproduce the discontinuous nature of the bricks or stones. The level of discretization is restricted by the desired size of the scaled model since blocks which are too small do not behave or interact with each other accurately. On the other hand, it is also incorrect to produce a monolithic scaled dome model. To readily produce a scaled model of the Hagia Sophia, while preserving finer details, this investigation chose to use 3D printed blocks (Zessin et al. 2010; Quinonez et al. 2010; Zessin 2012). The process workflow summarized in Figure (5) describes the inputs required to discretize a complete dome geometry into a series of blocks which can directly be printed. A similar logic to section 3.3.3, using Grasshopper and Python, was used. The blocks were printed with a ZCorp 450 gypsum powder printer and coated with a layer of polyurethane adhesive (Quinonez et al. 2010). This produces blocks that are durable through repeated testing and that have a suitable friction coefficient between them.

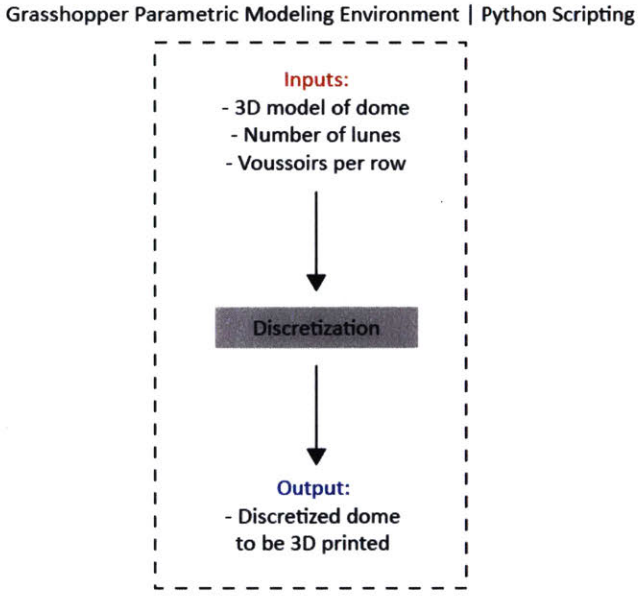

Figure (5): Process logic for discretization of 3D dome geometry into blocks to allow for printing of scaled geometry.

3.5 - Tilting Test

3.5.1 - Theory and Physical Implementation

Tilt testing is an experimental technique in which a masonry structure is placed on a planar surface which is gradually inclined until the structure collapses (DeJong 2009). This collapse angle can be linked to the minimum ground acceleration necessary to cause the collapse of the dome, a quasi-dynamic evaluation of the strength of an earthquake.

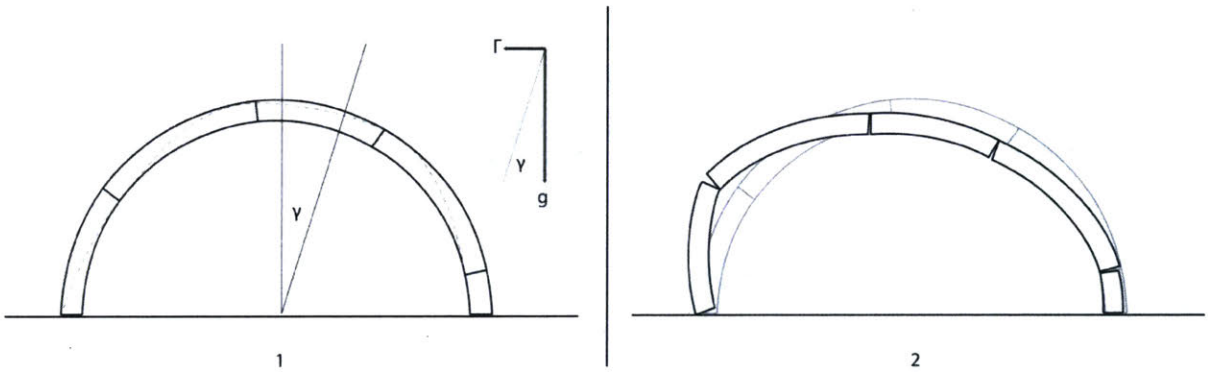

Figure (6): Tilting of an idealized hemispherical dome (1) and corresponding failure mechanism (2).

As demonstrated in Figure (7), tilting the dome causes the thrust line to lie tangent to the structure in 5 locations. As postulated by the Uniqueness Theorem in section 2.3, since this thrust line will cause hinges to form at this location, it is sufficient to cause the collapse of the structure. Thus, at a given angle of inclination corresponding to collapse, the thrust line will lie tangent to the dome and then exit the structure, indicating failure, due to hinging mechanisms. The relationship between the angle of collapse and ground acceleration can be computed based on a vector decomposition (DeJong 2009; Zessin 2012).

$$\Gamma = \tan(\gamma) * g \qquad \textbf{Equation 3.5.1}$$

3.5.2 - Validation

The results of the physical tilt table test can also be verified by adjusting the force polygon from section 3.3.3. By rotating the load line by the desired angle, a new force polygon corresponding to an inclined geometry can be found. This updated force polygon naturally links to a new thrust line which can be verified to make sure it still passes through the structure. The angle at which the thrust line is no longer admissible is the angle of collapse.

It is important to note that this modification of the force polygon can only be implemented if hoop forces are not considered (i.e. only meridional forces). As a result, a lower bound or conservative estimate of the collapse angle is achieved. This is because the specific implementation of graphic statics that considers hoop forces constrains the thrust line to the centerline of the lune.

3.6 - Spreading Test

3.6.1 - Theory and Physical Implementation

The spreading support test experimentally simulates the behavior of a masonry dome with supports that are displacing outwards either due to the thrust of the dome, weakness in adjacent structure, or differential soil settlement underneath the piers.

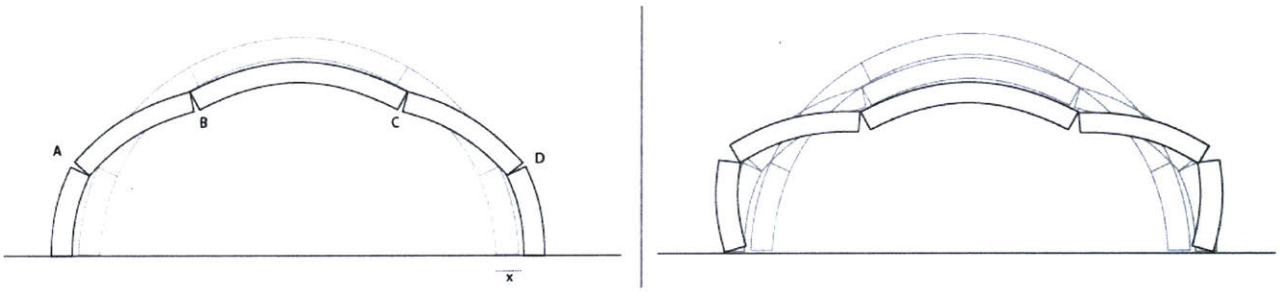

Figure (7): Spreading of an idealized hemispherical dome. The formation of 4 hinges indicates a failure mechanism. When the structure fails, two more hinges will form at the supports.

This displacement similarly shifts the line of thrust so that it lies tangent to the dome at the location of the four hinges (A, B, C, and D). When the actual collapse mechanism is induced, two more hinges will form at the base of the piers. Since the scaled model behaves in a similar way, it can be assumed that the displacement measured in the physical experiments can be magnified to describe the failure of the actual dome (Zessin et al. 2010; Zessin 2012).

3.6.2 - Validation

Analytic validation of the displacement necessary to cause collapse can be calculated by assuming that the dome is hemispherical and with a uniform thickness. For the Hagia Sophia, this will naturally be an upper bound for the actual displacement necessary to cause failure as the dome is much shallower and thinner than a corresponding hemispherical approximation. The formulaic derivation of the critical percentage span increase is given by the following equation (Zessin 2012).

$$\frac{2x_{crit}}{L} = -334\left(\frac{t}{R}\right)^2 + 283\left(\frac{t}{R}\right) - 10.7 \qquad \textbf{Equation 3.6.2}$$

In this expression, $\frac{2x_{crit}}{L}$ corresponds to the critical span increase while $\frac{t}{R}$ is the thickness to radius ratio of the dome. When applied to the Hagia Sophia, assuming a constant thickness of 2.4m which corresponds to the base of the pier, and a radius of approximately 16m, a predicted span increase of 23.9% (3.83m) would induce collapse.

IV - Results and Discussion

Based on the methodology presented in section 3, the analytical and experimental study of the dome of the Hagia Sophia was performed to demonstrate its static stability and its behavior under seismic loading and support displacement.

4.1 - Comparison of Hoop and Meridional Forces

One key question related to the static stability of the Hagia Sophia, and perhaps giving much insight into the behavior of domes in general, is the relative effect of hoop forces in the force equilibrium of the dome. Assuming a density of 1700 kg/m^3 (which is consistent with the FEM analysis of the dome) and a 10 degree lune with 11 voussoirs, values for the horizontal and vertical thrust were calculated for the dome of the Hagia Sophia. These are provided in Table (1).

Table (1): Thrust Values for the Dome of the Hagia Sophia

	No Hoop Forces	**Hoop Forces**
Horizontal Thrust (kN)	254	275
Vertical Thrust (kN)	1012	1012

Considering hoop forces does not make any difference with regards to the vertical thrust of the dome. Indeed, hoop forces simply flatten the thrust line slightly resulting in a higher horizontal thrust value if the hoop force calculation constrains the solution to the dome centerline. This is further illustrated by looking at the thrust lines for the two different conditions (see Figure (8)).

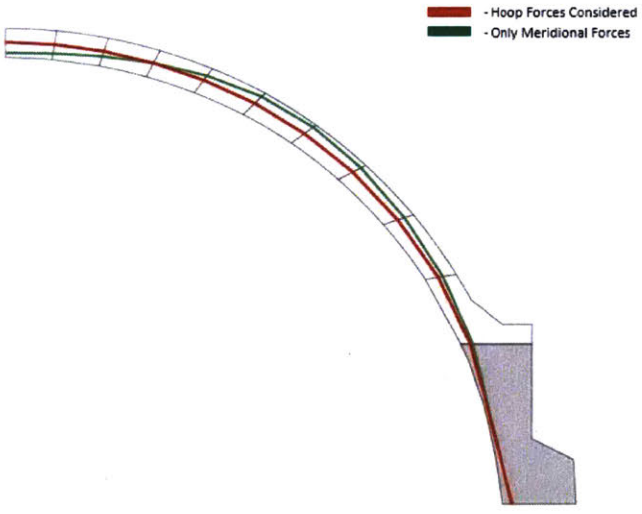

Figure (9): Thrust lines for the Hagia Sophia with and without hoop forces. The conditions are very similar. The thrust line which considers hoop forces is locked to the centerline of the dome since this is a critical assumption involved in the graphic statics technique.

It is evident that for the geometry of the dome of the Hagia Sophia, the two graphic statics methods yield similar results, albeit the consideration of hoop forces is a more realistic case for the static equilibrium of the structure.

4.2 - Overturning Stability of the Dome of the Hagia Sophia

An important metric for determining the stability of the Hagia Sophia is the safety of factor associated with the stability of the pier. In this calculation (see Figure (9)), it is assumed that the structure adjacent to the dome is very stiff and that the supporting pier is the most likely to overturn. A simple analysis of the stabilizing and overturning moments due to the thrust entering the pier reveals a very high safety factor against overturning as can be seen in Table (2).

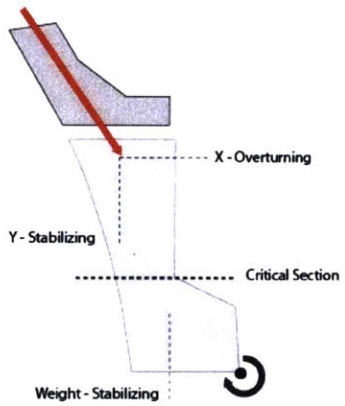

Figure (9): The pier of the Hagia Sophia may overturn due to the thrust imparted from the rest of the dome. It's resistance to overturning can be quantified as a safety factor. The thinnest part of the pier, the critical section, is highlighted.

Table (2): Safety Factor against Overturning for Piers of the Hagia Sophia Dome

	No Hoop Forces	**Hoop Forces**	**Hoop Forces (Crit. Section)**
Safety Factor against Overturning	2.02	1.90	1.06

The high stability is due to the large weight and volume of the pier which was most likely overdesigned and strengthened through the lifetime of the building for this exact purpose. When considering hoop forces, the safety factor decreases since there is an increased horizontal component of the thrust. When looking at the thinnest critical section of the pier, the safety factor further decreases to 1.06, due to the reduced section which is able to provide less resistance to overturning.

4.3 - Comparison to Other Methods

In order to validate the results of this investigation, it is important to compare the thrust values calculated using graphic statics to those that have previously been found using both membrane analysis and FEM analysis. With a density of 1700 kg/m^3, the FEM analysis of the dome produced a value of 600 kN for the vertical thrust and 154 kN for horizontal thrust (Swan and Cakmak 2010). This is half the value found using graphic statics and further diminishes the viability of using elastic analysis to study historic masonry structures. However, membrane theory, which operates on similar assumptions to graphic statics, can be used to study masonry domes. The membrane analysis of the dome of the Hagia Sophia, assuming a density of 1834 kg/m^3, yielded a vertical thrust value of 1069 kN and a horizontal thrust value of 267 kN (Duppel 2009). These results are nearly identical to those found in this investigation. While, membrane analysis may be used in lieu of graphic statics, this investigation has demonstrated that a flexible implementation of graphical methods can make the analysis of complex dome geometries quicker and more efficient without the need to develop governing equations and equilibrium conditions.

4.4 - Comparison to Later Ottoman Domes

Since the Hagia Sophia is considered the architectural and structural progenitor of all later Ottoman imperial mosques, it is important to analyze its static stability compared with two of the hallmarks of Ottoman construction, the Suleymaniye and Selimiye. The Suleymaniye was built in Istanbul under the orders of Sultan Suleiman I by Sinan from the years 1550-1558. The dome measures approximately 26 meters in diameter. The Selimiye, designed and built by Sinan from 1568-1574 in Edirne, is considered the pinnacle of Ottoman architecture and measures a staggering 32 meters in diameter, nearly identical to the Hagia Sophia. The 3D models for the two Ottoman domes were based on section cuts of the mosques. Both the Suleymaniye and Selimiye utilize flying buttresses to resist the outward spread of the dome. However, as indicated by the thrust lines in Figure (10), the two Ottoman domes are in static equilibrium even without the buttresses.

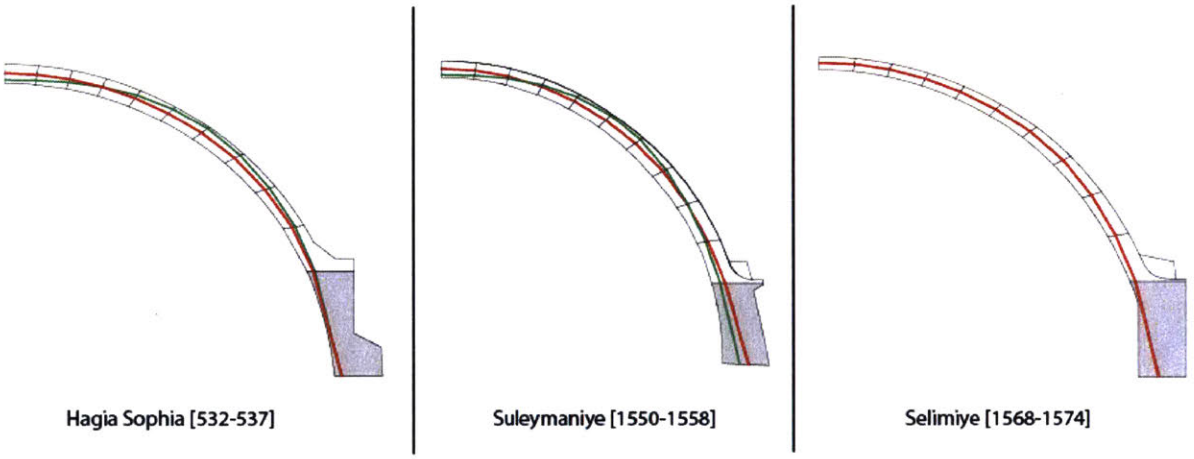

Figure (10): Thrust lines for the Hagia Sophia, Suleymaniye, and Selimiye. The thrust line which corresponds to only meridional forces is shaded green while the thrust line which also includes hoop forces is colored red.

It is important to note that while the Suleymaniye is stable considering solely meridional forces or including hoop forces, the thinner Selimiye requires hoop forces to be in static equilibrium. As a result, there is no admissible meridional force only thrust line that passes through its structure. In general, the thickness to radius ratio of the three domes is similar. The Hagia Sophia has a t/R = 0.148, the Suleymaniye has a t/R = 0.167, and the Selimiye has a t/R = 0.151. This metric only considers the thickness at the base of the pier but indicates that the aspect ratio of the domes is fairly similar indicating both architectural and structural continuity. The safety factors and thrust values, assuming hoop forces are present, for the three domes is summarized in Table (3). To compare geometry rather than materiality, the same 1700 kg/m^3 density was used to determine the self-weight of the domes.

Table (3): Static Stability and Thrust of the Hagia Sophia and Ottoman Domes

	Vertical Thrust (kN)	Horizontal Thrust (kN)	Safety Factor
Hagia Sophia	1011	274	1.90
Suleymaniye	719	200	1.73
Selimiye	1055	256	1.71

It is important to note the reduced safety factor associated with the two Ottoman mosques. Although the values are still higher than 1.5, concern about static stability may have driven Sinan to deploy flying

buttresses to prevent overturning and outward displacement. This is particularly evident in looking at the Selimiye, which is directly comparable to the Hagia Sophia in geometry and size. Even though it has a larger pier and less horizontal thrust (it is slightly less shallow than the Hagia Sophia), the safety factor is reduced by about 10% owing to the thinner size of the dome and the pier geometry.

4.5 - Collapse Due to Seismic Activity

The model of the dome of the Hagia Sophia was 3D printed at a 1:88 scale based on logistical constraints. This resulted in a dome with 10 rows of voussoirs and more than 100 3D printed pieces with a total span of approximately 46cm.

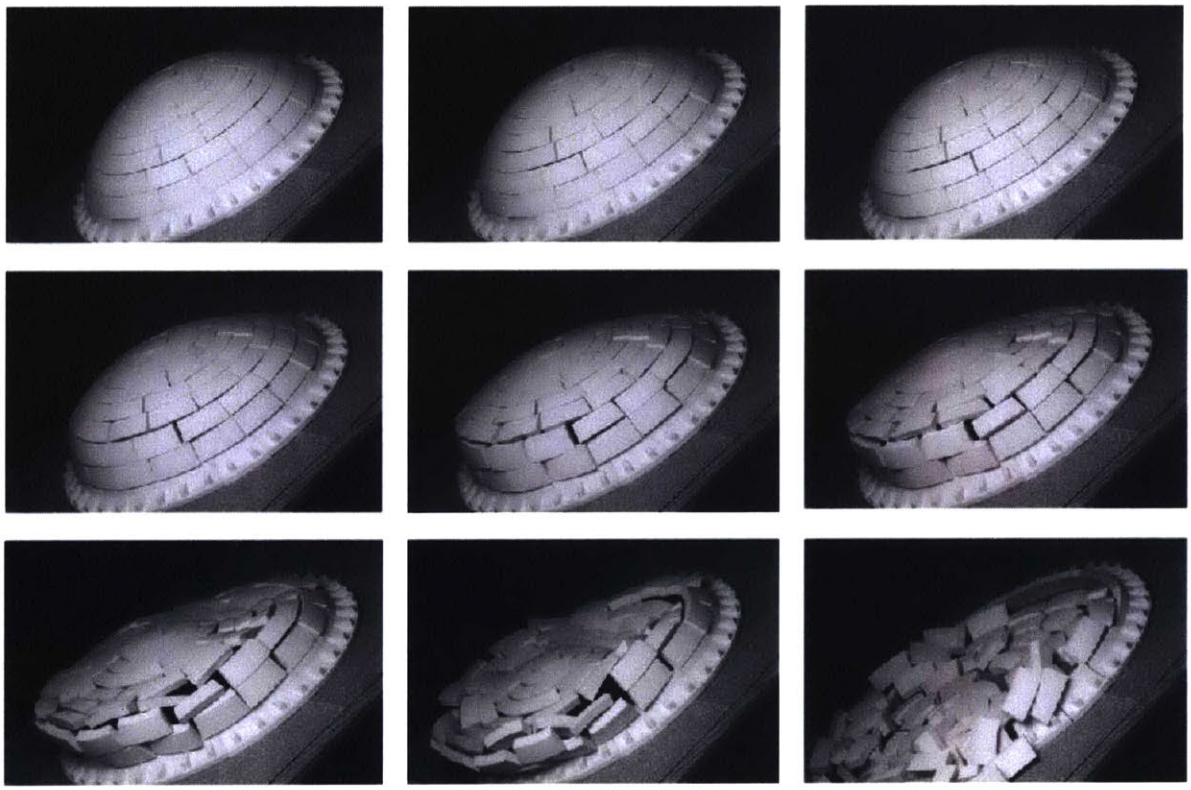

Figure (11): Collapse of the scaled model of the Hagia Sophia due to tilting to simulate seismic behavior.

The dome was placed on an inclined surface which was gradually tilted upwards until collapse was reached. The results were recorded using a high speed camera and are shown in Figure (11). As expected based on the method outlined in Section 3.5.1, the dome collapsed when 4 hinges form. The collapse induces a bulging of the dome in one direction and a flattening on the other side. Based on the angle of collapse recorded (35.9°), an average minimum ground acceleration of 0.725g (standard deviation of 0.031g) was determined using Equation 3.5.1 (see Table (4)).

Table (4): Experimental Values of Lateral Ground Acceleration Using Tilting Test

Test	**1**	**2**	**3**	**4**	**5**
Collapse Angle	36.7°	37.4°	36.3°	35.2°	34.1°
Acceleration	0.745g	0.765g	0.732g	0.705g	0.677g

The recorded collapse angle corresponds to a very high lateral ground acceleration and is indicative of the highly stable dome of the Hagia Sophia which is to be expected given the resilience of the building to withstand seismic activity over the last 1000 years. The trend for the last three tests lowers due to corner rounding and global damage to the blocks as a result of multiple collapses.

Apply the modified graphic statics method described in Section 3.5.2, a minimum ground acceleration of 0.51g is predicted. This is corresponding to an angle of 27°. At this state (see Figure (12)), the thrust line lies tangent to the lune at two different points and then exits the structure at the base. The thrust line is tangent at the crown and at a point located approximately 55° from the vertical. These tangencies correspond to the hinges that will form and cause a collapse mechanism.

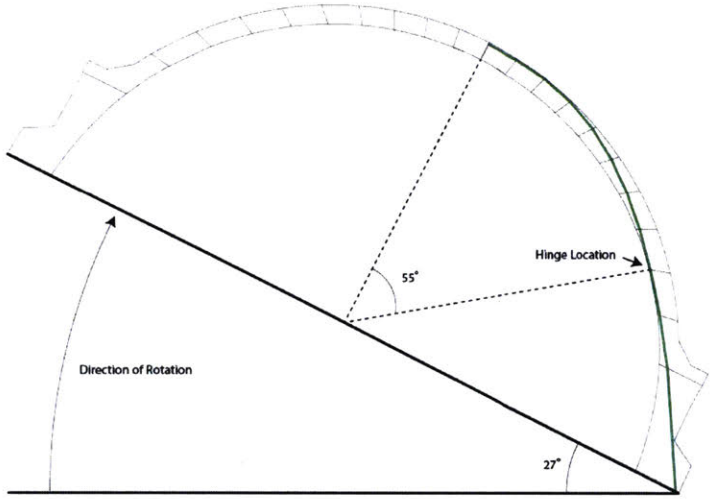

Figure (12): Analytical derivation of the angle of collapse of the Hagia Sophia using a modified graphic statics method. The green thrust line lies tangent to the lune at two points. The lower tangency corresponds to the formation of a hinge that causes a failure. This is the last admissible thrust line, indicating that this the highest angle at which the structure can be titled before failure is recorded.

This analytical derivation validates the experimental results since the graphical method is a lower bound, conservative estimate that does not consider hoop forces which are evidently influencing the behavior of the scaled model. In addition, the physical experiment also introduced friction between the blocks, which reduces their likelihood to rotate or hinge. However, the graphical method is unable to capture this. However, as can be seen from the still frames in Figure (11), the location of the hinge (between the second and third row of blocks) corresponds exactly to the position predicted using graphic statics.

Present-day Istanbul is located in a seismically active region and it is situated close to the North Anatolian fault. Based on historical data and seismic models, the Peak Ground Acceleration (PGA) for Istanbul is between 0.20g and 0.30g for earthquake events with a 10% likelihood in 50 years. For earthquakes with a 2% likelihood, the PGA is between 0.33g and 0.49g (Kalkan et al. 2008). These values indicate that although the region is expected to experience moderate to large seismic events, it is highly unlikely that the dome of the Hagia Sophia will collapse as a result, since a minimum lateral ground acceleration of 0.725g is required to induce a collapse mechanism in the structure.

Accelerometers installed throughout the Hagia Sophia (including the dome) record the response of the structure to seismic events and registered two large earthquakes that struck the region in 1999. The 7.4 magnitude Kocaeli earthquake occurred in August while the 7.2 magnitude Duzce earthquake occurred in November of that year. The peak acceleration recorded at the Hagia Sophia, during both events, was 0.077 m/s^2, or 0.0078g. (Durukal et al. 2003). This is significantly lower than the acceleration required to

cause collapse and thus, the Hagia Sophia is determinately safe during medium to large seismic events, as demonstrated by the two most recent, significant earthquakes.

4.6 - Collapse Due to Displacement of Supports

The scaled model of the dome of the Hagia Sophia was also placed on a spreading supports table to simulate the collapse mechanism associated with outward moving supports (Zessin et al. 2010; Zessin 2012). A series of 6 leaves are slowly moved apart and the movement of the dome is recorded with a high speed camera.

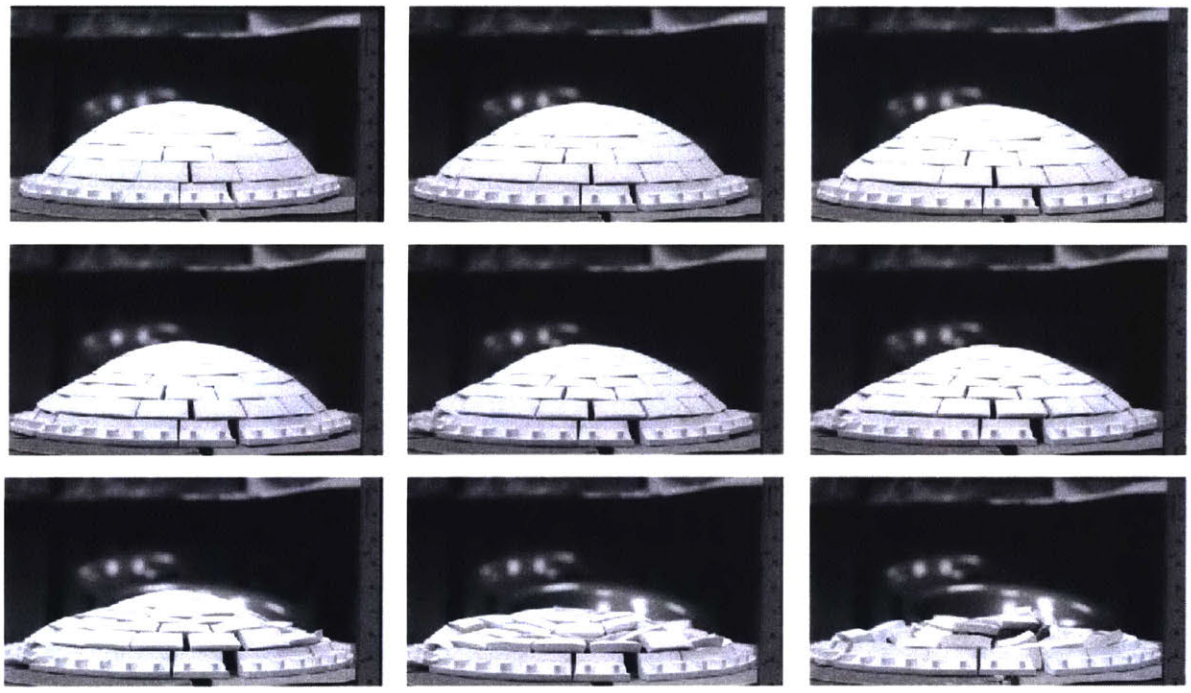

Figure (13): Collapse of the scaled model of the Hagia Sophia due to spreading supports.

On average, full collapse occurred after an average outward support movement of 2.4 cm (standard deviation of 0.15 cm) and a downward crown displacement of 0.6 cm (see Table(5)). Taking the scaling factor into account, this corresponds to 2.1m and 1.4m, respectively. The spreading supports first introduce cracks into the lower part of the dome. In these regions, the masonry cannot bear the tensile hoop forces present and the classical dome cracking pattern becomes visible. The upper part of the dome however, remains rigid with minimal cracking since there are compressive forces in this region. The dome ultimately only collapses when two hinges form per lune, or four hinges for any given cross section of the dome.

Table (5): Experimental Values for the Outward Spread Distance Required to Cause Dome Collapse

Test	**1**	**2**	**3**	**4**
Spreading Distance (cm)	2.54	2.22	2.38	2.54
Span Increase	10.0%	8.9%	9.4%	10.0%

This experimental result can be compared to a theoretical prediction by simplifying the dome to be purely hemispherical and uniform in thickness. As previously demonstrated, using Equation 3.6.2, a critical span increase of 23.8% is estimated to cause collapse in a hemispherical dome with a thickness to radius ratio of 0.148. Of course this is a non-conservative estimate of how far the supports of the Hagia Sophia can displace without causing failure mechanisms. Indeed, there is a 45% difference in the values corresponding to this simplified version of the dome versus the actual 3D printed geometry. The dome of the Hagia Sophia gets thinner towards the top and it is shallower than a hemispherical dome with the same diameter. Although the theoretical prediction serves as an upper bound estimate of performance, it is not refined enough to take into account specific geometric parameters. This result illustrates the significance and value of scaled physical models and necessitates the development of more rigorous analytical expressions to describe the stability behavior of domes.

V - Conclusions

The Hagia Sophia is a testament to the design and engineering prowess of Byzantine builders. Indeed, the iconic form was emulated closely by later Ottoman builders such as Sinan during the 16th century. The Hagia Sophia has stood, albeit in reconstructed and often rebuilt forms, for almost 1500 years however, little is understood about the stability of the building and its surprising resiliency in seismic events. As the signature part of the structure, the brick masonry dome of the Hagia Sophia is particularly interesting due to its long span and low thickness to radius ratio. This investigation aimed to better understand the fundamental behavior of the dome of the Hagia Sophia as a way to motivate appropriate restoration and conservation of this dome and other ancient and medieval masonry structures.

By developing an automated implementation of graphic statics, an adaptation of limit analysis which follows the fundamental stability governed behavior of masonry structures, this investigation was able to determine the relative magnitude of forces found throughout the dome. Accounting for hoop forces, the Hagia Sophia has a vertical thrust of 1011 kN and a horizontal thrust of 274 kN. These results can be corroborated with other structural analysis evaluations of the dome. For example, using membrane analysis, Duppel (2009) predicted a vertical thrust of 1069 kN and a horizontal thrust of 267. The results also help illustrate why computational FEM analysis, based on elastic strength criteria, are not well suited for analyzing masonry structures. Indeed, using FEM analysis, Swan and Cakmak (2010) estimated a vertical thrust of 600 kN and a horizontal thrust of 154 kN for the dome. It can be seen due to its geometry, the effect of radial hoop forces are not significant in the equilibrium state of the dome of the Hagia Sophia. This is different than later Ottoman domes which require hoop forces for their stability, such as the Selimiye in Edirne. Furthermore, using graphic statics, the investigation was able to validate the high resistance of the dome piers from overturning due to thrust from the dome. Considering its thickest section, the dome pier has a 1.90 factor of safety against overturning. Even considering the thinnest section of the piers, the factor of safety against overturning remains adequate, with a value of 1.06.

Building on previous work with discretized, physical masonry models, this investigation 3D printed and collapse tested a scaled model of the dome of the Hagia Sophia. This model, again based on the principles of limit analysis, assumes that the blocks or masonry units are rigid bodies and that collapse is a result of plastic hinge formation rather than failure due to material strength. Considering the dome on a titling surface, the minimum lateral ground acceleration necessary to induce collapse was found to be 0.725g. This high value points to the resiliency of the current dome configuration and its ability to withstand multiple seismic events in the past centuries. The safety of the dome can be further confirmed by comparing this value to the expected PGA in Istanbul of 0.33g to 0.49g. Finally, by looking at the dome on spreading supports, this investigation demonstrated that a minimum 2.1 meter movement of the piers is required to induce a collapse mechanism in the dome. Both these experimental values can be validated by considering theoretical approximations of the two collapse states.

Further refinement of this investigation can focus on both the experimental and analytical portions of the study. To more fully understand the seismic behavior of the Hagia Sophia, more of the structure can be 3D printed and tested, including the supporting piers. In addition, by using laser-scanning tools on site, a more complete and accurate geometry of the building and dome can be generated which will further refine the 3D model used for both experimentation and graphic statics and make any conclusions more directly relevant to the actual building. Finally, a future iteration of this investigation

can focus on rigorously establishing theoretical expressions for the stability and quasi-dynamic behavior of non-hemispherical, non-uniform thickness domes. These general expressions would be instrumental in the analysis of the Hagia Sophia as well as any other historical masonry dome.

Through a combination of automated, graphic methods and physical, scaled models, this investigation has developed a robust methodology to analyze the stability of non-hemispherical, non-uniform thickness masonry domes and evaluate their seismic and support behavior via quasi-dynamic experimental testing. This process has indeed shown the applicability and advantages of limit analysis to analyze heritage masonry structures and has revealed significant insights into the behavior of the dome of the Hagia Sophia.

VI - Appendix A

A.1. Graphic Statics Theory and Implementation

As a specific implementation of limit analysis, graphic statics is a technique that correlates external loads with internal actions, via vector equilibrium.

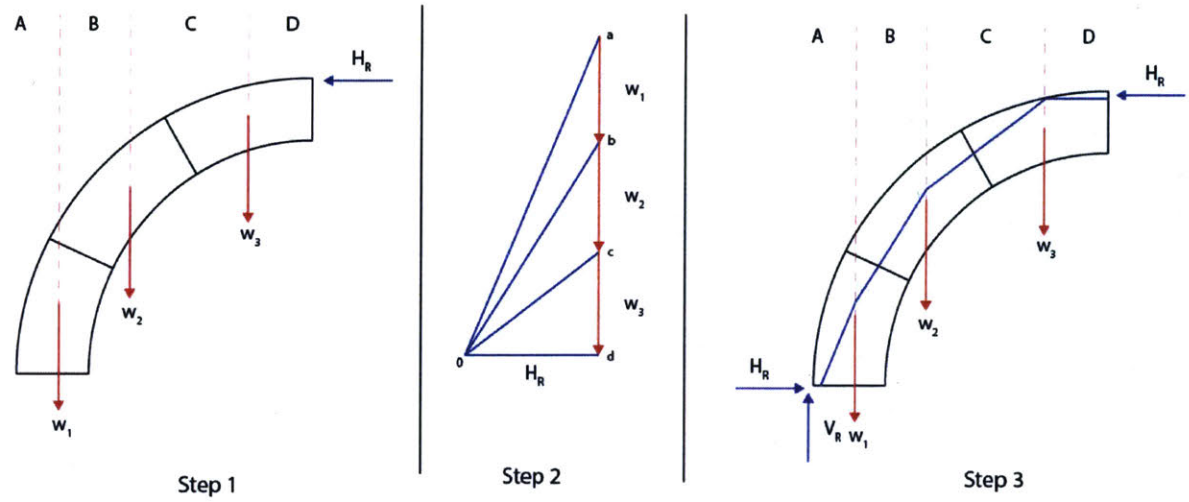

Figure (A1): The three steps involved in generating the thrust line for a given geometry. Here, a state of minimum thrust is displayed. This forms the basic premise of graphic statics and can be expanded from a 2D arch into more complex geometries

Figure (A1) illustrates the basic premise involved with generating the thrust line for a 3 *voussoir* (segment) arch in two dimensions (unit depth into the page) (Allen and Zalewski 2009). The first step involves determining the forces acting on the masonry structure. In the case of the given example, the only load present is the self-weight of each voussoir (w_1, w_2, and w_3) which can be represented by downward vectors with a given scaled magnitude. It is important that the scaling factor used to draw forces in graphic statics is kept constant. In step 2, the vectors representing the self-weight of the blocks are placed tip to tail in a vertical representation which is called the *load line*. Picking a point (the *node* or o) horizontal with regards to the beginning of the load line will establish the horizontal reaction force necessary to keep the arch in equilibrium. By connecting the tips of the load vectors to the node, the arch is now in equilibrium. This graphical representation is called a *force polygon*. The magnitude of the lines (*a-o, b-o, c-o, d-o*) correspond to the magnitude of the meridional force in that voussoir of the arch (when the necessary scaling factor is applied). As step 3 demonstrates, lines with the same slopes can be then be drawn within the geometry of the arch. This is the thrust line for the structure. If the thrust line fits wholly within the geometry, it is an admissible equilibrium solution and the arch is stable. As is instantly noticeable, there are a large number of admissible thrust lines which can be generated, even for a simple arch. Different equilibrium conditions can be found by moving the node location to the left or right, thereby decreasing or increasing the magnitude of the horizontal reaction at the crown of the arch and redefining the thrust line.

VII - Appendix B

B.1. Lune Generation and Voussoir Discretization

```
import rhinoscriptsyntax as rs
import math
import Rhino as rh
from Grasshopper.Kernel.Data import GH_Path
from Grasshopper import DataTree
import scriptcontext as sc
import Rhino.Geometry as rg

sc.doc = rh.RhinoDoc.ActiveDoc
rh.RhinoDoc.ActiveDoc.ModelAbsoluteTolerance = 0.001;

angleDomeTree = DataTree[object]();
vertDomeTree = DataTree[object]();
finalDomeTree = DataTree[object]();
radialDivisionsTree = DataTree[object]();
world_Z = [0,0,1];
world_Y = [0,1,0];
inputGeo = Input_Geo;
centPoint = Center_Point

if Run:
    angle_Vert = Lune_Angle;
    #centPoint = [0,0,0]
    #centPoint = rs.SurfaceVolumeCentroid(inputGeo[0]);
    #centPoint = centPoint[0]
    vertDivGuide = rs.AddLine(centPoint,(0,100,centPoint[2]));

    angle_updated1 = 0;
    angle_updated2 = angle_Vert[0]

    xform_1 = rs.XformRotation2(angle_updated1,world_Z,centPoint);
    xform_2 = rs.XformRotation2(angle_updated2,world_Z,centPoint);

    vertDivLine_Array_1 = rs.TransformObject(vertDivGuide,xform_1,True);
    vertDivLine_Array_2 = rs.TransformObject(vertDivGuide,xform_2,True);

    join_vertDivLine = rs.JoinCurves([vertDivLine_Array_1,vertDivLine_Array_2],True);

    vertCuttingSurfaces_1 =
rs.ExtrudeCurveStraight(join_vertDivLine,centPoint,[0,0,100]);
    vertCuttingSurfaces_2 = rs.ExtrudeCurveStraight(join_vertDivLine,centPoint,[0,0,-
100]);
    vertCuttingSurfaces =
rs.JoinSurfaces([vertCuttingSurfaces_1,vertCuttingSurfaces_2],True);

    brp_1 = rs.coercebrep(vertCuttingSurfaces);
    brp_2 = rs.coercebrep(inputGeo[0]);

    rs.FlipSurface(brp_1);

    brp_vert = rh.Geometry.Brep.CreateBooleanDifference(brp_2,brp_1,0.001);

    angle_count = Angled_Div[0];

    angleDivLine = rs.AddLine([0,0,0],[0,100,0]);
    angleDiv_indx = [90/i for i in Angled_Div]
    angleDiv = [];
    angleDivLine_2D = [];
```

```
    angleDivLine_polar = [];
    angleCutSurfaces = [];
    angleCutDome = []
    anglebrepGeo = brp_vert[0];
    newLine = rs.AddLine([0,0,0],[0,0,1])
    radialDivisions = [];

    angleCutSurfaces.append(rs.AddRevSrf(angleDivLine,newLine,0,360));

    for i in range(0,angle_count):
        angleDiv.append(angleDiv_indx[0]*i+angleDiv_indx[0]);

angleDivLine_2D.append(rs.RotateObject(angleDivLine,[0,0,0],angleDiv[i],None,True));

angleDivLine_polar.append(rs.RotateObject(angleDivLine_2D[i],[0,0,0],90,world_Y,False)
);
        angleCutSurfaces.append(rs.AddRevSrf(angleDivLine_polar[i],newLine,0,360));

        anglebrepSrf = rs.coercebrep(angleCutSurfaces[i]);

        brp_3 =
rh.Geometry.Brep.CreateBooleanDifference(anglebrepGeo,anglebrepSrf,0.01);

        rs.FlipSurface(anglebrepSrf,True);

        brp_4 =
rh.Geometry.Brep.CreateBooleanDifference(anglebrepGeo,anglebrepSrf,0.01)

        rs.FlipSurface(anglebrepSrf,True);

        anglebrepGeo = brp_4[0]
        print brp_4

        angleCutDome.append(brp_3);
        path_1 = GH_Path(i)
        angleDomeTree.AddRange(angleCutDome[i],path_1);

        radialDivisions.append(rs.coercecurve(angleDivLine_polar[i]));

    angleCutDome.append(brp_4);
    path_2 = GH_Path(angle_count+1)
    angleDomeTree.AddRange(angleCutDome[angle_count],path_2);

    Lune = angleDomeTree
    radialDivisions.insert(0,rs.coercecurve(angleDivLine));
    Radial_Divisions = radialDivisions;

    rs.DeleteObjects(angleCutSurfaces);
    rs.DeleteObjects(angleDivLine_2D);
    rs.DeleteObjects(angleDivLine);
    rs.DeleteObjects(angleDivLine_polar);
    rs.DeleteObjects(newLine);

rs.DeleteObjects([vertCuttingSurfaces,join_vertDivLine,vertDivGuide,vertDivLine_Array_
1,vertDivLine_Array_2]);

sc.doc = ghdoc;
```

B.2. Graphic Statics Only Considering Meridional Forces

```
import rhinoscriptsyntax as rs
import Rhino as rh
import itertools as iter
from Grasshopper.Kernel.Data import GH_Path
from Grasshopper import DataTree
import math as m

length = len(Input_Vsr_Geo);
forceLen = [];
forceLine = [];
fPolygPt = Init_Pt_ForcePolyg;

for i in range(0,length):
    vsrGeo = rs.coercebrep(Input_Vsr_Geo[i]);
    volVoussoir = rs.SurfaceVolume(vsrGeo);
    forceLen.append(volVoussoir[0]*Density/Force_Scale);

startPt = fPolygPt;
cumsums = [sum(forceLen[:i+1]) for i in xrange(len(forceLen))];
cumsums.insert(0,fPolygPt[2]);

forceLine = [];
angledPoints = [];

for i in range (1,length):
    angledPoints.append([0,fPolygPt[1]-(cumsums[i]*m.tan(Tilt_Angle)),cumsums[i]]);
angledPoints.insert(0,[0,fPolygPt[1],fPolygPt[2]]);

for i in range (1,length):
    tilt_point = angledPoints[i];
    endPt = [0,tilt_point[1],tilt_point[2]];
    forceLine.append(rs.AddLine(startPt,endPt));
    startPt = endPt;

forceLine.insert(length,rs.AddLine(endPt,[0,fPolygPt[1]-
(cumsums[length]*m.tan(Tilt_Angle)),cumsums[length]]));

horzPoint = [0,Horz_Rct_Slider,cumsums[length]];
forcePolyg = [];
vectPolyg = [];
unit_vectPolyg = [];

for i in range (0,length):
    tilt_point = angledPoints[i];
    forcePolyg.append(rs.AddLine([0,tilt_point[1],tilt_point[2]],horzPoint));
    vectPolyg.append(rs.VectorCreate([0,tilt_point[1],tilt_point[2]],horzPoint));
    unit_vectPolyg.append(rs.VectorUnitize(vectPolyg[i]));

horzLine = rs.AddLine([0,fPolygPt[1]-
(cumsums[length]*m.tan(Tilt_Angle)),cumsums[length]],horzPoint);

forcePolyg.insert(length,horzLine);

disp_fpolyg = [forcePolyg,forceLine];
fpolygTree = DataTree[object]();

for i in range (0,len(disp_fpolyg)):
    path_fpolyg = GH_Path(i);
    fpolygTree.AddRange(disp_fpolyg[i],path_fpolyg);
```

```
unit_vectPolyg.reverse();
unit_vectPolyg[:] = [x*-1 for x in unit_vectPolyg]

Force_Polyg = fpolygTree;

startPt_TL = Init_Pt_ThrustLine;
thrustLine = [];
TL_scale = 2;

Radial_Divisions.pop();
Radial_Divisions.reverse()
Radial_Divisions.insert(len(Radial_Divisions)+1,Drum_Curve);

for i in range (0,length):
    thrustLine.append(rs.AddLine(startPt_TL,startPt_TL+unit_vectPolyg[i]*TL_scale));
    intersectTL = rs.LineLineIntersection(thrustLine[i],Radial_Divisions[i]);
    start_nextTL = intersectTL[0];
    thrustLine[i] = rs.AddLine(startPt_TL,start_nextTL);
    startPt_TL = start_nextTL;

Thrust_Line = thrustLine
```

B.3. Graphic Statics Considering Hoop and Meridional Forces

```
import rhinoscriptsyntax as rs
import Rhino as rh
import itertools as iter
from Grasshopper.Kernel.Data import GH_Path
from Grasshopper import DataTree
import ghpythonlib.components as ghc
import math as m

length = len(Input_Vsr_Geo);
forceLen = [];
forceLine = [];
fPolygPt = Init_Pt_ForcePolyg;
brepFaces = [];
zeroHF = Zero_Hoop_Force;

for i in range(0,length):
    vsrGeo = rs.coercebrep(Input_Vsr_Geo[i]);
    volVoussoir = rs.SurfaceVolume(vsrGeo);
    forceLen.append(volVoussoir[0]*Density/Force_Scale);

for i in range (0,length):
    expBrep = ghc.DeconstructBrep(Input_Vsr_Geo[i]);
    if len(expBrep.faces) > 6:
        mergeBrep = ghc.MergeFaces(Input_Vsr_Geo[i])
        expBrep = ghc.DeconstructBrep(mergeBrep)
        brepFaces.append(expBrep.faces[4]);
    else:
        brepFaces.append(expBrep.faces[2])

averageLine = [];
vect_averageLine = [];
unit_vectaverageLine = [];

for i in range (0,length):
    brepEdges = ghc.BrepEdges(brepFaces[i]);
    edgeLen = ghc.Length(brepEdges.naked);
    sortEdge = ghc.SortList(edgeLen,brepEdges.naked);
    line_1 = sortEdge._1[0];
    line_2 = sortEdge._1[1];
    cut_1 = ghc.DivideCurve(line_1,2);
    cut_2 = ghc.DivideCurve(line_2,2);
    midPt_1 = cut_1.points[1];
    midPt_2 = cut_2.points[1];
    averageLine.append(rs.AddLine(midPt_1,midPt_2));
    vect_averageLine.append(rs.VectorCreate(midPt_1,midPt_2));
    unit_vectaverageLine.append(rs.VectorUnitize(vect_averageLine[i]));

startPt = fPolygPt;
cumsums = [sum(forceLen[:i+1]) for i in xrange(len(forceLen))];
cumsums.insert(0,fPolygPt[2]);

forceLine = [];
angledPoints = [];

for i in range (1,length):
    angledPoints.append([0,fPolygPt[1]-(cumsums[i]*m.tan(Tilt_Angle)),cumsums[i]]);
angledPoints.insert(0,[0,fPolygPt[1],fPolygPt[2]]);

for i in range (1,length):
    tilt_point = angledPoints[i];
```

```
    endPt = [0,tilt_point[1],tilt_point[2]];
    forceLine.append(rs.AddLine(startPt,endPt));
    startPt = endPt;

forceLine.insert(length,rs.AddLine(endPt,[0,fPolygPt[1]-
(cumsums[length]*m.tan(Tilt_Angle)),cumsums[length]]));

horzPoint = [0,Horz_Rct_Slider,cumsums[length]];
forcePolyg = [];
vectPolyg = [];
unit_vectPolyg = [];

for i in range (0,zeroHF):
    tilt_point = angledPoints[i];
    forcePolyg.append(rs.AddLine([0,tilt_point[1],tilt_point[2]],horzPoint));
    vectPolyg.append(rs.VectorCreate([0,tilt_point[1],tilt_point[2]],horzPoint));
    unit_vectPolyg.append(rs.VectorUnitize(vectPolyg[i]));

horzLine = rs.AddLine([0,fPolygPt[1]-
(cumsums[length]*m.tan(Tilt_Angle)),cumsums[length]],horzPoint);

forcePolyg.insert(length,horzLine);
intersectPt = [];

for i in range (zeroHF,length):
    tilt_point = angledPoints[i];
    pointInit = rs.coerce3dpoint([0,tilt_point[1],tilt_point[2]]);
    pointMove = pointInit + unit_vectaverageLine[i]*-500;
    lineExtend = rs.AddLine(pointInit,pointMove);
    lineIntersect = rs.LineLineIntersection(horzLine,lineExtend);
    intersectPt.append(lineIntersect[0]);
    forcePolyg.append(rs.AddLine(lineIntersect[0],pointInit));
    vectPolyg.append(rs.VectorCreate(lineIntersect[0],pointInit));
    unit_vectPolyg.append(rs.VectorUnitize(vectPolyg[i]));

HF_1 = [];
HF_2 = [];

angle = ghc.Radians(Lune_Angle);
intersectPt = ghc.ReverseList(intersectPt);
intersectPt.insert(0,rs.coerce3dpoint([0,fPolygPt[1]-
(cumsums[length]*m.tan(Tilt_Angle)),cumsums[length]]));
lenHF = len(intersectPt);

vectNeg = rs.coerce3dvector([0,m.tan(angle)*-1,1]);
vectPos = rs.coerce3dvector([0,m.tan(angle),1]);

index = 0;
while index < lenHF-1:
    pointMove_HF_neg = intersectPt[index] + vectNeg*500;
    pointMove_HF_pos = intersectPt[index+1] + vectPos*500;
    lineExtend_HF_neg = rs.AddLine(intersectPt[index],pointMove_HF_neg);
    lineExtend_HF_pos = rs.AddLine(intersectPt[index+1],pointMove_HF_pos);
    lineIntersect_HF = rs.LineLineIntersection(lineExtend_HF_pos,lineExtend_HF_neg);
    HF_1.append(rs.AddLine(intersectPt[index],lineIntersect_HF[0]));
    HF_2.append(rs.AddLine(intersectPt[index+1],lineIntersect_HF[0]));
    index = index + 1;

disp_fpolyg = [forcePolyg,forceLine,HF_1,HF_2];
fpolygTree = DataTree[object]();

for i in range (0,len(disp_fpolyg)):
    path_fpolyg = GH_Path(i);
```

```
    fpolygTree.AddRange(disp_fpolyg[i],path_fpolyg);

Force_Polyg = fpolygTree;

startPt_TL = Init_Pt_ThrustLine;
thrustLine = [];
TL_scale = 2;

unit_vectPolyg = ghc.ReverseList(unit_vectPolyg);

Radial_Divisions.pop();
Radial_Divisions.reverse()
Radial_Divisions.insert(len(Radial_Divisions)+1,Drum_Base);

for i in range (0,length):
    thrustLine.append(rs.AddLine(startPt_TL,startPt_TL+unit_vectPolyg[i]*TL_scale));
    intersectTL = rs.LineLineIntersection(thrustLine[i],Radial_Divisions[i]);
    start_nextTL = intersectTL[0];
    thrustLine[i] = rs.AddLine(startPt_TL,start_nextTL);
    startPt_TL = start_nextTL;

Thrust_Line = thrustLine
```

VIII – Bibliography

Almac, U., Schweizerhof, K., Blankenhorn, G., Duppel, C., and Wenzel, F. (2013). Structural behavior of the Hagia Sophia under dynamic loads. *Vienna Congress on Recent Advances in Earthquake Engineering 2013 (VEESD 2013)*.

Allen, E. and W. Zalewski (2009). *Form and Forces: Designing Efficient, Expressive Structures*. New York: John Wiley & Sons.

Block, P. (2005). *Equilibrium Systems: Studies in Masonry Structure.* S.M. thesis, Department of Architecture, Massachusetts Institute of Technology, Cambridge, Massachusetts.

Cakmak, A.S., Davidson, R., Mullen, C.L., and Erdik, M. (1993). Dynamic analysis and earthquake response of Hagia Sophia. *Transactions on the Built Environment 3*, 881-898.

Cakmak, A.S., Moropoulou, A., and Mullen, C.L. (1995). Interdisciplinary study of dynamic behavior and earthquake response of Hagia Sophia. *Soil Dynamics and Earthquake Engineering 14*, 125-133.

Culmann, C. (1864). *Die graphische Statik*. Zurich: Verlag von Meyer & Zeller.

DeJong, M.J (2009). *Seismic Assessment Strategies for Masonry Structures*. Ph.D. thesis, Department of Architecture, Massachusetts Institute of Technology, Cambridge, Massachusetts.

Duppel, C. (2009). *Ingenieurwissenschafliche Untersuchugen an der Hauptkuppel un den Hauptfeilern der Hagia Sophia in Istanbul*. Ph.D. Thesis, Faculty of Architecture, Karlsruhe Institute of Technology, Karlsruhe, Germany.

Durukal, E. Cimilli, S., and Erdik, M. (2003). Dynamic response of two historical monuments in Istanbul deduced from the recordings of Kocaeli and Duzce earthquakes. *Bulletin of the Seismological Society of America, 93(2)*, 694-712.

Heyman, J. (1997). *The Stone Skeleton: Structural Engineering of Masonry Architecture*. Cambridge University Press, Cambridge.

Kalkan, E., Gulkan, P., Yilmaz-Ozturk, N., Celebi, M. (2008). Seismic hazard in the Istanbul metropolitan area: a preliminary re-evaluation. *Journal of Earthquake Engineering 12,* 151-164.

Lau, W.W. (2006). *Equilibrium Analysis of Masonry Domes*. S.M. thesis, Department of Architecture, Massachusetts Institute of Technology, Cambridge, Massachusetts.

Mark, R., and Cakmak, A.S. (1992). *The Hagia Sophia: From the Age of Justinian to the Present*. Cambridge University Press, Cambridge.

Mark, R., and Cakmak, A.S. (1994). Mechanical Tests of Material from the Hagia Sophia. *Dumbarton Oaks Papers 48*, 277-278.

Mark, R., Cakmak, A.S., Hill, K., and Davidson, R. (1995). Structural analysis of Hagia Sophia: a historical perspective. *Transactions on the Built Environment 4*, 33-46.

Necipoglu, G. (2005). *The Age of Sinan: Architectural Culture in the Ottoman Empire*. Reaktion Books, London.

Poleni, G. (1748). *Memorie istorische della Gran Cupola del Tempio Vaticano*. Padova: Nella Stamperia del Seminario.

Plunkett, J.W. (2016). *The Roman Pantheon: Scale-Model Collapse Analyses*. S.M. thesis, Department of Architecture, Massachusetts Institute of Technology, Cambridge, Massachusetts.

Quinonez, A., Zessin, J., Nutzel, A., Ochsendorf, J. (2010). Small-Scale Models for Testing Masonry Structures. *Advanced Materials Research 133-134,* 497-502.

Robert McNeel and Associates (2014). *Grasshopper 3D Version 0.9.0076.* Seattle, Washington.

Robert McNeel and Associates (2012). *Rhinoceros 3D Version 5.0*. Seattle, Washington.

Swan, C.C. and Cakmak A.S. (1993). Nonlinear quasi-static and seismic analysis of the Hagia Sophia using an effective medium approach. *Soil Dynamics and Earthquake Engineering 12*, 256-271.

Wolfe, W.S. (1921). *Graphical Analysis: A Text Book on Graphic Statics*. McGraw-Hill Book Company, New York.

World Monuments Fund (2017). A Closer Look: Hagia Sophia. https://www.wmf.org/project/hagia-sophia

Zessin, J.F., Lau, W.W, and Ochsendorf, J.A. (2010). Equilibrium of cracked masonry domes. *Engineering and Computational Mechanics 163*, 134-145.

Zessin, J.F. (2012). *Collapse Analysis of Unreinforced Masonry Domes and Curving Walls*. Ph.D. thesis, Department of Architecture, Massachusetts Institute of Technology, Cambridge, Massachusetts.